Technical Memorandum No. 33-201

Viscous Damping of Roll During Entry of a Mars Entry and Landing Capsule

Jack E. Marte

Bain Dayman, Jr.

Bain Dayman, Jr., Chief
Aerodynamic Facilities

JET PROPULSION LABORATORY
CALIFORNIA INSTITUTE OF TECHNOLOGY
PASADENA, CALIFORNIA

April 1, 1965

Prepared Under Contract No. NAS 7-100
National Aeronautics & Space Administration

CONTENTS

TABLE

FIGURES

ABSTRACT

2 6 1 4 7

An analysis has been made of the viscous damping in roll of two capsule configurations during planetary entry. The analysis extends the incompressible solution of flow over a rotating flat disk to the region behind the bow shock of both a blunt and a hemisphere-cone forebody. The results of a simplified example show the damping to be about 7%, independent of the initial roll rate. A method of integrating the results into the six-degree of freedom program has been developed.

I. INTRODUCTION

The reduction of capsule roll rate due to viscosity in the boundary layer is an aerodynamic effect not presently included in the six-degree of freedom planetary entry program. This effect may indirectly play a significant part in the dynamic behavior of the pitch and yaw degrees of freedom. Additionally, a point could be reached where the roll rate becomes equal to the transverse oscillation frequency leading to an uneven distribution of heat input on the heat shield. This memorandum presents a summary of an analytical investigation into some aspects of the problem along with the results of a simplified example to indicate the magnitude of the effect.

II. ANALYSIS

In Ref. 1–3 Schlichting and Truckenbrodt investigated the problem of rotational damping due to an incompressible flow over a rotating flat disk. This analysis extends their results to the subsonic region behind a normal bow shock produced by a blunt body during an entry trajectory. An additional extension, to a poorer approximation, is made to the essentially conical flow around a blunted conical shape. The configurations under discussion are shown in Fig. 1. The results apply strictly to zero angle of attack and aerodynamically smooth surfaces. In accordance with a statement by Schlichting (Ref. 4) that regions of separated flow contribute little to the damping torque, only the forebody is considered effective in damping the roll rate. Although Schlichting and Truckenbrodt presented results for both laminar and turbulent boundary layers, no attempt to predict transition on the nose was made. The boundary layer was conservatively assumed turbulent throughout the entry trajectory in the example. The laminar equations are included for reference purposes.

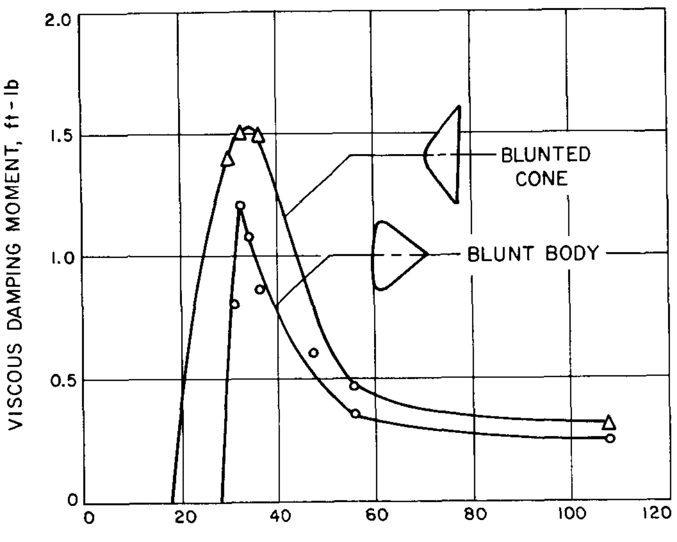

Fig. 1. Variation of viscous damping moment with entry time for blunt body and blunted cone

In Ref. 2 Truckenbrodt gives as the equation for damping moment coefficient on a flat disk with a turbulent boundary layer

$$C_T = \frac{0.079}{(Re)^{0.2}}\left(\frac{U}{Rp}\right)^{0.8} \quad (1)$$

The roll rate is p, R the disk radius, U the free stream velocity (here the velocity behind the shock) and $Re = R^2p/\nu$ where ν is the kinematic viscosity. Equating the postshock velocity to the free stream velocity of Ref. 2 is an approximation made in the interests of simplicity. It is not inconsistent with the overall degree of approximation of the analysis. The equivalent expression for the laminar boundary layer case, as given in Ref. 3 by Schlichting and Truckenbrodt, is

$$C_T = \frac{2.53}{(Re)^{0.5}}\left(\frac{U}{Rp}\right)^{0.5} \quad (2)$$

Knowing this coefficient, the damping moment on a rotating disk can be calculated from

$$T = \left(\frac{\rho}{2}\right) p^2 R^5 C_T \quad (3)$$

The functional dependence of the damping moment on the flow variables for the turbulent and laminar cases is

$$T_{TURB} = 0.040p\, \rho^{0.8} R^{3.8} U^{0.8} \eta^{0.2} \quad (4)$$

$$T_{LAM} = 1.27p\, \rho^{0.5} R^{3.5} U^{0.5} \eta^{0.5} \quad (5)$$

where η is absolute viscosity and, ρ is density—both evaluated behind the shock wave.

In the numerical calculations, the atmospheric parameters were taken from a trajectory computed by Peter Feitis on August 21, 1964 for the following entry conditions

Planet	Mars
Atmosphere	M69-2
Entry angle	−90 deg
Entry velocity	24,000 ft/sec
Entry latitude	0 (equatorial)
Capsule ballistic coefficient	$M/C_DA = 0.2$ slug/ft²
Trajectory program	3 deg of freedom

The procedure in making the computation was to assume a roll rate and moment of inertia about the roll axis, and calculate the damping moment using Eq. 1 and 3 or 6 at a series of points along the trajectory. The atmospheric parameters from the three-degree of freedom program were used to obtain flow conditions behind the bow shock for the normal shock case or at the body surface for the conical flow case. These values of the flow parameters were substituted into Eq. (1) for the roll damping coefficient. The resulting value of C_T was then used to obtain the damping moment. As a first approximation the roll rate used in these computations was assumed constant; although if damping occurs, the value used at each succeeding point will decrease. It is shown below that this approximation does not substantially affect the magnitude of the effect.

In the blunt body case the values of density, temperature, and velocity immediately behind the normal shock were used in the calculation for simplicity although stagnation values of the flow parameters exist at the center of the nose and vary radially. Trial calculations using stagnation values as a limiting case produced insufficient increase in damping moment to warrant an approximation of the radial temperature and density distribution.

Kopal's tables (Ref. 5) were used to obtain surface values for density and temperature on the blunted cone. The temperature ratio across the shock was estimated as the value behind a normal shock using the Mach number component normal to the oblique shock as the upstream Mach number. In addition to the altered flow around the conical shape, as compared to the disk, it was necessary to account for the increased surface area of a cone over a disk of the same radius. This was simply accomplished by modifying Eq. 3 as shown below

$$T = \frac{\rho p^2 R^5 C_T}{2 \sin\varphi} \tag{6}$$

where φ is the cone apex half-angle.

The results of the calculations are shown in Fig. 1 where the damping moment is plotted against time (since atmospheric entry at 800,000 ft) for both disk and cone cases. The figure shows that the damping moment of the cone is somewhat greater than the disk but that both have the same general shape. The damping moments for the disk, as computed using stagnation density and temperatures, fell between the two curves shown in Fig. 1. Here the disk case, as previously described, was based on flow parameters behind the normal shock. Maximum damping moments occurred at quite high altitudes because the compression ratio across the shock (increasing Mach number) increases with altitude. This more than compensates for the decrease of atmospheric density with altitude up to 80,000 ft.

Knowing the variation of damping moment with time, the damping of the roll rate can be obtained by integration of the rotary equation of motion,

$$T = -I \frac{dp}{dt} \tag{7}$$

I is the moment of inertia about the roll axis and t the elapsed time. The negative relationship occurs because the damping moment always has a sense opposite to $d\theta/dt = p$ where θ is the angle of roll.

$$\frac{dp}{dt} = -\frac{T}{I} \tag{8}$$

To simplify the integration in the example, the cone curve of Fig. 1 was approximated by linear segments as shown in Fig. 2. The functional dependence of the damping moment on time for the curve of Fig. 2 can be written as

$$T(t) = T + Kt \tag{9}$$

where K is the slope of the curve in Fig. 2. Substitution of Eq. (9) in Eq. (8) yields

$$\frac{dp}{dt} = \frac{T + Kt}{I} \tag{10}$$

which, on integration, produces

$$p = p_i - \frac{1}{I}\left[Tt + \frac{K}{2}t^2\right] \tag{11}$$

This is the required relationship between roll velocity and time.

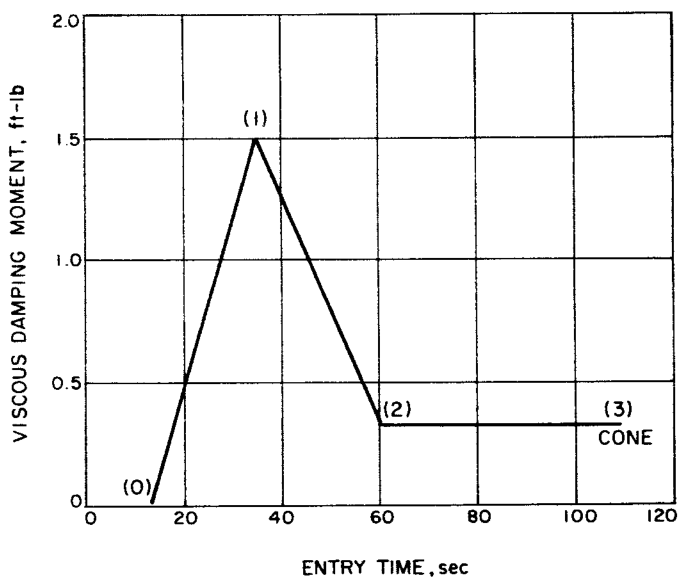

Fig. 2. Linearized viscous damping moment versus entry time curve for blunted cone

III. RESULTS

Using an initial roll rate of 100 rpm ($p_i = 10.49$ rad/sec) and $I = 76$ slug/ft², the following values for p at the points indicated in Fig. 2 are obtained for the cone case.

Table 1. Roll rate at selected points on entry trajectory

Point	*t*, sec	*K*, ft-lb/sec	*p*, rad/sec	p/p_i
0	0	—	10.49	1.000
1	22	0.0682	10.27	0.979
2	25	−0.0472	9.97	0.950
3 (impact)	48	0	9.77	0.931

In other words, the roll rate of the cone case is reduced about 7% due to viscous damping during the entry, and the assumption of constant p in computing the ρ vs. t curve was approximately correct. Variation in the initial roll rate produces proportional variation in subsequent roll rates so the ratio to the initial value remains as given in Table 1. This follows from Eq. (4) or (5) which shows the damping moment to be proportional to the roll rate and from the fact that the roll rate at any time is the integral of the damping moment curve over that time period.

Since the kinetic energy of a rotating body is

$$E = \tfrac{1}{2} I p^2 \tag{12}$$

the energy lost due to skin friction during entry is

$$\begin{aligned} \Delta E &= E_0 - E_3 \\ &= \frac{I}{2}(p_0^2 - p_3^2) = p_0^2\left[1 - \left(\frac{p_3}{p_0}\right)^2\right] \\ &= 554 \text{ ft-lb} \end{aligned} \tag{13}$$

for the values of p_0 and I used above. The subscripts 0 and 3 indicate beginning of entry and impact, respectively. This represents about 13% of the original rotary kinetic energy. The term within the square brackets in Eq. (13) is independent of the initial roll rate; so the energy loss is proportional to the square of the initial roll rate. For example, an initial roll rate of 10 rpm would result in a loss of rotational energy of 1.3% of the original value.

IV. APPLICATION

In order to apply the results of this analysis to computer programs, such as the Ames six-degree of freedom program, it is necessary to convert to standard stability notation in which the rolling moment

$$T = C_l\,(qsR) = C_l\left(\frac{\rho}{2}\cdot U^2 \cdot \pi R^3\right) \tag{14}$$

When this is equated to Eq. (4) or (5), expressions for C_l in terms of the flow and geometric variables are obtained for the turbulent and laminar cases respectively as

$$C_{l_{\text{TURB}}} = 0.255\,\frac{p\,R^{0.8}\,v^{0.2}}{U^{1.2}} \tag{15}$$

$$C_{l_{\text{LAM}}} = 0.808\,\frac{p\,R^{0.5}\,v^{0.2}}{U^{1.5}} \tag{16}$$

The roll damping coefficient C_{l_p} is defined as

$$C_{l_p} = \frac{dC_l}{d\left(\frac{pR}{U}\right)}$$

and it is in this form that the damping moment enters the six-degree of freedom program. In the aerodynamic moment equation about the x-body axis as given in section 5, page 17, of Ref. 11, the equation is modified by the addition of the damping term to read (in program notation of Ref. 11)

$$M_{AXB} = -F_{AZB}\,\varepsilon_y + F_{AYB}\,\varepsilon_z + C_{l_p}\,\frac{\overline{Q}\,sd^2p}{V_A} \qquad (17)$$

$$\begin{bmatrix}\text{product of}\\ z\text{-force and}\\ \text{moment arm}\end{bmatrix}\begin{bmatrix}\text{product of}\\ y\text{-force and}\\ \text{moment arm}\end{bmatrix}\begin{bmatrix}\text{damping}\\ \text{term}\end{bmatrix}$$

This term differs from pitch (or yaw) damping by reason of the fact that the effect here is due to the action of viscosity. Therefore, as shown by Eq. (15) and (16), C_l and C_{l_p} are functions of both Mach number and viscosity (altitude). In the turbulent case, the viscosity effect causes a change during entry of about $\pm 15\%$ in the value of C_l from a mean value while in the laminar case the change is about twice that amount. With some prior information of the trajectory (such as a three-degree of freedom trajectory) the relationship between Mach number and altitude may be considered sufficiently well known to tabulate required density and viscosity and velocity values behind the bow shock as functions of Mach number alone. These tables can then be entered as inputs in computing $C_l = f(M)$ for use in the main program.

V. DISCUSSION

Aerodynamic flow tables and tables of gas properties for gas mixtures similar to the Martian atmosphere are quite limited, especially at hypersonic Mach numbers and for conical flow. Those tables and curves available (Ref. 5–9) were used as best they could be in approximating the flow conditions. Where possible the 9% CO_2 – 91% N_2 tables of Ref. 5 were used, but for the conic flow Kopal's tables for $\gamma = 1.405$ were, of necessity, used. In some instances it was possible to make comparisons between values calculated by various means, and in those cases the resulting differences did not seriously affect the final results. For example, a comparison of density and temperature ratios between $\gamma = 1.405$ and $\gamma = 1.67$ for which limited tables are given in Kopal showed a 6% increase in torque for the laminar case and a 3% decrease in the turbulent case for $\gamma = 1.67$. This variation is within the accuracy of the calculation itself, and the applicable specific heat ratio for the planetary atmosphere ($\gamma = 1.38$) is considerably closer to $\gamma = 1.405$ than was the comparison value so that the variation of torque will be even less. The quantity known to the least accuracy was probably the viscosity in the hypersonic regime, but fortunately this term occurs in the moment equation [Eq. (4)] to the 0.2 power. The controlling term among the flow variables appeared to be the density.

The approximation of conical flow around the blunted cone was considered quite reasonable in spite of the fact that this shape has a blunt nose which produces a normal bow wave in the vicinity of the axis of rotation. This is true because the greater part of damping moment lies in the region where the bow wave is much nearer to the conical configuration than to a normal shock.

As mentioned earlier, this analysis was made for bodies with detached flow behind the forebody. If a configuration on which the flow remains attached behind the forebody is to be investigated, the contribution of such an afterbody will have to be considered. There appear to be no difficulties in extending this analysis to those configurations by computing the afterbody contribution separately from the nose and adding the two to obtain the net effect. In fact, experimental work, principally at NOL, has been done on slender bodies at low supersonic Mach numbers.

Pitching oscillations of small amplitude will probably not greatly change the damping moment until they reach the point where the flow over the nose separates on the downstream side. Under those conditions, experimental measurements would be required. Increasing roughness on the nose of the body will certainly increase the damping moment. Slight increases in surface roughness might require no more than an experimentally determined change in the value of the constant in Eq. (1) or perhaps a change in the exponents of the other terms of that equation. The general approach of this analysis should remain applicable with increasing roughness, but changes in the parameters of the governing equation may have to be determined experimentally. The results of systematic experiments on the effect of roughness of skin friction coefficient have been published by F. Goddard and others.

VI. CONCLUSIONS

An order of magnitude analysis of the reduction of roll rate due to viscous effects produced a reduction of 7% as a maximum (a 13% decrease in roll kinetic energy) during entry in the M 69-2 atmosphere. In view of the approximations of flow conditions behind the shock it may not be warranted to include a 7% effect in the six-degree of freedom program until such a time as flow tables for CO_2-N_2 atmospheres into the hypersonic regime are available. Further work on roll damping with roughness would be justified if said roughness can be sufficiently characterized.

REFERENCES

1. Schlichting, H., and E. Truckenbrodt, "The Flow Around a Rotating Disc in a Uniform Stream," *Journal of Aeronautical Sciences*, September, 1951.

2. Truckenbrodt, E., "Die turbulente Strömung an einer angeblasenen Rotierenden Scheibe" (The Flow over a Rotating Flat Plate with Turbulence), *Zeitschrift für angewandte Mathematik und Mechanik,* Vol. 34, 1954, p. 150.

3. Schlichting, H., and E. Truckenbrodt, "Die Strömung an einer angeblasenen rotierenden Scheibe" (The Flow over a Rotating Flat Plate), *Zeitschrift für angewandte Mathematik und Mechanik,* Vol. 32, 1952, p. 97.

4. Schlichting, H., *Boundary Layer Theory*, McGraw-Hill Book Co., Inc., New York, 1955.

5. Kopal, Z., *Tables of Supersonic Flow Around Cones*, Technical Report No. 1, Massachusetts Institute of Technology, Department of Electrical Engineering, Center of Analysis, Cambridge, Massachusetts, 1947.

6. Peterson, W., *Tables of Flow Properties of Thermally Perfect Carbon Dioxide and Nitrogen Mixtures*, National Aeronautics and Space Administration, SP-3009, 1964.

7. Ames Research Staff, *Equations, Tables, and Charts for Compressible Flow*, National Advisory Committee for Aeronautics, Report 1135, Washington, D. C., 1953.

8. Hansen, F., and S. Heims, *A Review of Thermodynamic, Transport and Chemical Reaction Rate Properties of High-Temperature Air*, National Advisory Committee for Aeronautics, TN 4359, Washington, D. C., July, 1958.

9. Lewis Computing Staff, *Tables of Various Mach Number Functions for Specific-Heat Ratios from* 1.28 *to* 1.38, National Advisory Committee for Aeronautics, TN 3981, Washington, D. C., April, 1957.

10. Gruszczynski, J., and W. Warren, "Hypervelocity Heat Transfer Studies in Simulated Planetary Atmospheres," Paper No. 63-450, *American Institute of Aeronautics and Astronautics*, Vol. 1, 1963.

11. Snyder, D., "Six Degree of Freedom Program for Studying Motions of Vehicles Entering Planetary Atmospheres," (private communication with Don Snyder).